Effects of ligand planarity on the interaction of polypyridyl Ru(II) complexes with DNA

Hong Xu,[a,b] Kang-Cheng Zheng,*[a,c] Yao Chen,[d] Yi-Zhi Li,[d] Li-Jun Lin,[a,c] Hong Li,[e] Pei-Xin Zhang[b] and Liang-Nian Ji *[a,c]

[a] The Key Laboratory of Gene Engineering of Ministry of Education, Zhongshan University, Guangzhou 510275, P. R. China. E-mail: cesjln@zsu.edu.cn; Fax: 86-20-8403-5497; Tel: 86-20-8411-0115
[b] Department of Chemistry and Biology, Normal College, Shenzhen University, Shenzhen 518060, P. R. China
[c] Department of Chemistry, Zhongshan University, Guangzhou 510275, P. R. China
[d] State Key Laboratory of Coordination Chemistry, Nanjing University, Nanjing 210093, P. R. China
[e] Department of Chemistry, South China Normal University, Guangzhou 510631, P. R. China

Two new polypyridyl ligands containing substituent Br at different positions in the phenyl ring, OBIP {OBIP = 2-(2-bromophenyl)imidazo[4,5-*f*]-1,10-phenanthroline}, PBIP {PBIP = 2-(4-bromophenyl)imidazo[4,5-*f*]-1,10-phenanthroline} and their Ru(II) complexes, [Ru(dmp)$_2$(OBIP)]$^{2+}$ **1** and [Ru(dmp)$_2$(PBIP)]$^{2+}$ **2** (dmp = 2,9-dimethyl-1,10-phenanthroline), have been synthesized and characterized. The binding of the two complexes to calf thymus DNA (CT DNA) has been investigated by spectrophotometric methods, viscosity measurements, as well as equilibrium dialysis and circular dichroism spectroscopy. Theoretical calculations for the two complexes were also carried out applying the density functional theory (DFT) method. The structure of complex **1** has been determined by single-crystal X-ray diffraction techniques. The imidazo[4,5-*f*]-1,10-phenanthroline moiety is not coplanar with the 2-bromophenyl ring, having a dihedral angle of 48.6° in the OBIP ligand. The twisted conformation has been further confirmed by theoretical calculations, in which this dihedral angle is 48.2°. The theoretical calculations also suggest that the PBIP ligand in complex **2** is essentially planar (dihedral angle is 0.4°). The experimental results show that while complex **1** binds to CT DNA *via* a semi-intercalative mode, complex **2** strongly binds to CT DNA through intercalation. Complex **2** is thus a much better candidate as an enantioselective binder to CT DNA than complex **1**. Some experimental regularities or trends have been reasonably explained by the theoretical results. These suggest that the planarity of the intercalated ligand has significant effects on the spectral properties and the DNA-binding behavior of the complexes, and that the DFT method can be used effectively to explain and predict some regularities or trends in the interaction of polypyridyl Ru(II) complexes with DNA.

Introduction

Over the past decade, the interaction between transition metal complexes and DNA has been extensively studied.[1] In recent years, polypyridyl Ru(II) complexes have attracted much attention. As intercalating photoactive electron donors, polypyridyl Ru(II) complexes have been used to study DNA-mediated charge transport.[2] Some new technologies such as picosecond time-resolved resonance Raman spectroscopy and femtosecond linear dichroism spectroscopy have been applied to study DNA-binding geometries, binding modes and binding dynamics of polypyridyl Ru(II) complexes.[3] Increasing attention has also been given to the design of novel polypyridyl Ru(II) complexes which may be employed as probes of nucleic acid structures and sites.[4] Polypyridyl Ru(II) complexes can bind to DNA in a non-covalent interactive fashion such as electrostatic binding, groove binding[5] and intercalative binding (including classical intercalation,[6] semi-intercalation and quasi-intercalation [3f]). Many important applications of these complexes require that the complex binds to DNA through an intercalative mode. Generally the intercalative ligand of polypyridyl Ru(II) complex should contain an aromatic heterocyclic functionality that can insert and stack between the base pairs of double helical DNA.[1] Therefore most of the reported complexes contain only planar aromatic ligands and investigations of polypyridyl Ru(II) complexes with non-planar ligands as DNA-binding reagents have been relatively few. In fact, some of the complexes containing non-planar ligand also exhibit interesting properties upon binding to DNA.[7] Thus it is of interest to delineate the effects of the planarity of the intercalative ligand on interaction and the binding mode of complexes to DNA. In this paper, we selected OBIP {OBIP = 2-(2-bromophenyl)imidazo[4,5-*f*]-1,10-phenanthroline} and PBIP {PBIP = 2-(4-bromophenyl)imidazo[4,5-*f*]-1,10-phenanthroline} as intercalative ligands. The *ortho*-Br group shows a significant steric effect and can interact with N in OBIP, whereas the space constraint and such an N-interaction of the *para*-Br group in PBIP are negligible. As a result, the planarity of the two ligands could be different by selecting a suitable ancillary ligand.

To more clearly compare the effects of the planarity of the intercalative ligand on interaction of a complex with DNA, the selection of ancillary ligands is also very important. Ancillary ligands can also indirectly affect the DNA-intercalation state through changing the planarity of the main ligand. From the results of previous experiments,[8] dmp (dmp = 2,9-dimethyl-1,10-phenanthroline) can not intercalate into DNA and its methyl substituents are π-electron-pushing groups. It is with such considerations that leads us to select dmp as the ancillary ligands, and the complexes [Ru(dmp)$_2$(OBIP)]$^{2+}$ **1** and [Ru-(dmp)$_2$(PBIP)]$^{2+}$ **2** were thus selected for study. Since the four methyl substituents of the two ancillary ligands leads to an increase of electron density at the N and *ortho*-Br atoms in the main ligand OBIP, this will cause an increase of Coulombic repulsion between N and Br, and as a result, may lead to non-planarity of OBIP.

We report herein the syntheses and characteristics of two new polypyridyl ligands, OBIP and PBIP, and the corresponding Ru(II) complexes, [Ru(dmp)$_2$(OBIP)]$^{2+}$ **1** and [Ru-(dmp)$_2$(PBIP)]$^{2+}$ **2**, along with the crystal structure of complex **1** and examine their different DNA-binding behaviors. The theoretical calculations applying the density functional theory (DFT) method[9] for these two complexes were also carried out and applied to explain the obtained experimental observations. This paper is focused on exploring the effects of intercalated ligand planarity on the DNA-binding behavior and the spectral properties of the complexes.

Experimental

Syntheses

The complex cis-[Ru(dmp)$_2$Cl$_2$]·2H$_2$O and 1,10-phenanthroline-5,6-dione were prepared according to the literature procedures.[10] Other reagents and solvents were purchased commercially and used without further purification unless otherwise noted.

OBIP. OBIP was synthesized by a similar method described previously.[11] A mixture of 2-brombenzaldehyde (3.5 mmol, 0.40 cm^3), 1,10-phenanthroline-5,6-dione (2.5 mmol, 0.525 g), ammonium acetate (50 mmol, 3.88 g) and glacial acetic acid (10 cm^3) was refluxed for about 2 h, then cooled to room temperature and diluted with water (ca. 25 cm^3). Dropwise addition of concentrated aqueous ammonia gave yellow precipitates, which were collected and washed with water. The crude products were purified by silica gel filtration (60–100 mesh, ethanol). The principal yellow band was collected. The solvent was removed by rotary evaporation, the products were collected, and then dried at 50 °C in vacuo. Yield 0.727 g, 78% (Found: C, 60.57; H, 3.28; N, 14.80%. Calc. for C$_{19}$H$_{11}$BrN$_4$: C, 60.80; H, 2.93; N, 14.93%). ^{1}H NMR [(CD$_3$)$_2$SO]: δ 13.84 (s, 1H), 9.05 (d, 2H), 8.90 (d, 1H), 8.86 (d, 1H), 7.87 (q, 2H), 7.83 (d, 2H), 7.62 (t, 1H), 7.53 (t, 1H). m/z 375 and 377 (M$^+$).

PBIP. This compound was obtained using a procedure analogous to that for OBIP, using 4-brombenzaldehyde in place of 2-brombenzaldehyde. Yield 0.694 g, 74% (Found: C, 60.69; H, 3.31; N, 14.89%. Calc. for C$_{19}$H$_{11}$BrN$_4$: C, 60.80; H, 2.93; N, 14.93%). ^{1}H NMR [(CD$_3$)$_2$SO]: δ 13.56 (br, 1H), 9.03 (d, 2H), 8.92 (d, 2H), 8.25 (d, 2H), 7.82 (m, 4H). m/z 375 and 377 (M$^+$).

[Ru(dmp)$_2$(OBIP)](OH)(ClO$_4$)·CH$_3$CN 1. This complex was prepared by the following method. A mixture of cis-[Ru-(dmp)$_2$Cl$_2$]·2H$_2$O (0.5 mmol, 0.321 g), OBIP (0.5 mmol, 0.187 g), ethanol (10 cm^3) and water (5 cm^3) was refluxed under argon for 2 h to give a clear red solution. After most of the ethanol solvent was removed under reduced pressure, a red precipitate was obtained by dropwise addition of a saturated aqueous NaClO$_4$ solution. The product was purified by column chromatography on alumina using acetonitrile–toluene (1 : 1 v/v) as eluent and then dried in vacuo. Red prismatic single crystals of [Ru(dmp)$_2$(OBIP)](OH)(ClO$_4$)·CH$_3$CN were obtained by evaporating a solution of the complex in acetonitrile–toluene–water. Yield, 0.331 g, 63% (Found: C, 56.23; H, 3.62; N, 12.30%. Calc. for C$_{49}$H$_{39}$BrClN$_9$O$_5$Ru: C, 56.03; H, 3.72; N, 12.01%). ^{1}H NMR [(CD$_3$)$_2$SO]: δ 8.99 (d, 2H), 8.81 (d, 2H), 8.51 (t, 5H), 8.33 (d, 2H), 8.06 (d, 2H), 7.94 (d, 1H), 7.81 (d, 1H), 7.54 (t, 1H), 7.46 (d, 2H), 7.42 (m, 3H), 7.23 (br, 1H), 2.04 (s, 6H), 1.81 (s, 6H). m/z 893 ([M − OH$^-$ − ClO$_4$$^-$ − CH$_3$CN + 1]$^{2+}$).

[Ru(dmp)$_2$(PBIP)](ClO$_4$)$_2$ 2. This red complex was synthesized in a manner identical to that described for complex **1**, with 0.5 mmol, 0.187 g PBIP in place of OBIP. Yield, 0.359 g, 66% (Found: C, 52.04; H, 3.42; N, 10.33%. Calc. for C$_{47}$H$_{35}$BrCl$_2$N$_8$O$_8$Ru: C, 51.70; H, 3.21; N, 10.27%). ^{1}H NMR

[(CD$_3$)$_2$SO]: δ 8.90 (d, 2H), 8.74 (d, 2H), 8.42 (t, 4H), 8.23 (t, 4H), 7.96 (d, 2H), 7.62 (d, 2H), 7.37 (d, 2H), 7.33 (t, 2H), 7.13 (br, 2H), 1.94 (s, 6H), 1.71 (s, 6H). m/z 892 ([M − 2ClO$_4$$^-$]$^{2+}$).

The ligand, MBIP {MBIP = 2-(3-bromophenyl)imidazo-[4,5-f]-1,10-phenanthroline} and its Ru complex, [Ru(dmp)$_2$-(MBIP)]$^{2+}$ have also been synthesized with a analogous procedure described above. Unfortunately, the complex did not dissolve in water. Thus, unfortunately, we could not systematically study the effects of the planarity of the intercalative ligands containing Br-groups substituted at all the different position of the phenyl ring, on the binding mode of the complexes to DNA.

CAUTION: Perchlorate salts of metal complexes with organic ligands are potentially explosive, and only small amounts of the material should be prepared and handled with great care.

Crystallography

Crystal data and data collection parameters. C$_{49}$H$_{39}$BrClN$_9$-O$_5$Ru, M = 1050.31, monoclinic, space group $P2_1/c$ (no. 14), a = 11.526(1), b = 21.726(2), c = 18.124(1) Å, α = 90.00, β = 92.12(1), γ = 90.00°, U = 4535.4(6) Å^3, T = 293 K, Z = 4, μ(Mo-Kα) = 1.345 mm^{-1}, 22331 reflections measured, 7967 unique (R_{int} = 0.025) which were used in all calculations. The final $wR(F^2)$ was 0.0799 (all data).

Structure solution and refinement. Single crystal X-ray diffraction experiments were carried out with a Bruker Smart Apex CCD area detector in the range $1.87 < \theta < 25.00°$, $-13 \le h \le 13$, $0 \le k \le 25$, $0 \le l \le 21$, operating in ω scan mode and using graphite-monochromated Mo-Kα radiation (λ = 0.71073 Å). The reflection intensities were corrected by means of a ψ-scan. The structure was solved by direct methods and refined by full-matrix least-squares against F^2 of all data, using the SHELXTL 97 program.[12] All hydrogen atoms were generated geometrically (C–H 0.96 Å). 624 parameters were applied to refinement. The final difference map had peaks between −0.49 and 0.45 e Å^{-3}.

CCDC reference number 195053.

See http://www.rsc.org/suppdata/dt/b3/b300353a/ for crystallographic data in CIF or other electronic format.

Measurements

Elemental analyses (C, H and N) were carried out with a Perkin-Elmer 240C elemental analyzer. ^{1}H NMR spectra were recorded on a Bruker DRX-500 NMR spectrometer with (CD$_3$)$_2$SO as solvent and SiMe$_4$ as an internal standard. An LCQ electrospray mass specremeter (ESMS, Finnigan) was employed for the investigation of charged metal complex species in methanol solvent. UV-Vis spectra were recorded on a Shimadzu UV-2501PC spectrophotometer. Emission spectra were determined with a Shimadzu RF-5301PC fluorescence spectrometer. The circular dichroism spectra of dialyzates were measured on a JASCO J-715 spectropolarimeter.

Cyclic voltammetry was performed on an Autolab PGSTAT30 electrochemical system. The supporting electrolyte was 0.1 M tetrabutylammonium perchlorate in acetonitrile freshly distilled from phosphorus pentaoxide. All samples were purged with nitrogen prior to measurements at room temperature. The electrochemical measurements were made in a typical cell using a platinum wire working electrode, a platinum flat counter electrode, and a standard saturated sodium calomel electrode (SSCE).

All the experiments involving interaction of the complexes with DNA were conducted in twice distilled buffer containing tris(hydroxymethyl)aminomethane (Tris, 5 mM) and NaCl (50 mM) and adjusted to pH 7.2 with hydrochloric acid. A solution of calf thymus DNA in the buffer gave a ratio of UV absorbance at 260 and 280 nm of about 1.8–1.9:1, indicating that the

DNA was sufficiently free of protein.[13] The DNA concentration per nucleotide was determined by absorption spectroscopy using the molar absorption coefficient (6600 $M^{-1} cm^{-1}$) at 260 nm.[14]

For the absorption spectra, equal amounts of DNA were added to both complex and reference solutions to eliminate the absorbance of DNA itself. The intrinsic binding constant K_b of a complex to CT DNA was determined from eqn. (1)[15] through a plot of $[DNA]/(\varepsilon_a - \varepsilon_f)$ *vs.* [DNA].

$$\frac{[DNA]}{\varepsilon_a - \varepsilon_f} = \frac{[DNA]}{\varepsilon_b - \varepsilon_f} + \frac{1}{K_b(\varepsilon_b - \varepsilon_f)} \quad (1)$$

where [DNA] is the concentration of DNA in base pairs, ε_a, ε_f and ε_b are, respectively, the apparent extinction coefficient (A_{obs}/[M]), the extinction coefficient for free metal (M) complex and the extinction coefficient for the metal (M) complex in the fully bound form. In plots of $[DNA]/(\varepsilon_a - \varepsilon_f)$ *vs.* [DNA], K_b is given by the ratio of the slope to the intercept.

For the steady-state competitive binding experiment, according to the classical Stern–Volmer equation (2)[16]

$$I_0/I = 1 + Kr \quad (2)$$

where I_0 and I are the fluorescence intensities in the absence and presence of complex, respectively. K is a linear Stern–Volmer quenching constant dependent on the ratio of the bound concentration of ethidium bromide (EB) to the concentration of DNA; r is the ratio of the total concentration of the complex to that of DNA ([Ru]/[DNA]). In the plot of I_0/I *vs. r*, the Stern–Volmer quenching constant K is given by the ratio of the slope to the intercept.

Viscosity measurements were carried out using an Ubbdlodhe viscometer maintained at a constant temperature of 28.0 ± 0.1 °C in a thermostatic bath. DNA samples with an approximate average length of 200 base pairs were prepared by sonication in order to minimize complexities arising from DNA flexibility.[17] Flow time was measured with a digital stopwatch. Each sample was measured three times and an average flow time was calculated. Data are presented as $(\eta/\eta_0)^{1/3}$ *vs.* binding ratio ([Ru]/[DNA]),[18] where η is the viscosity of DNA in the presence of complex and η_0 is the viscosity of DNA alone. Viscosity values were calculated from the observed flow time of DNA-containing solutions ($t > 100$ s) corrected for the flow time of buffer alone (t_0), $\eta = t - t_0$.

The dialysis membrane was purchased from Union Carbide Co. and treated by means of the general procedure before use.[19] Equilibrium dialysis was carried out in the dark and held at 4 °C for 48 h with 5 cm^3 of calf thymus DNA (1.0 mM) sealed in a dialysis bag and 10 cm^3 of the complex (100 μM) outside the bag.

Theoretical calculations

Each of these two complexes forms from a Ru(II) ion, one main (intercalating) ligand (PBIP or OBIP) and two ancillary ligands (dmp). Full geometry optimization computations were preformed applying the DFT-B3LYP method[9] and LanL2DZ basis set,[20] and assuming the singlet state for the complexes.[21] All computations were performed with the G98 quantum chemistry program-package.[22] In order to vividly depict the detail of the frontier molecular orbital interactions, the stereographs of some related frontier molecular orbitals of the complexes were drawn with the Molden v3.6 program[23] based on the obtained computational results.

Results and discussion

Structures

The molecular structure of complex **1** has been confirmed by single crystal X-ray diffraction analysis. It consists of a

Table 1 Selected bond lengths (Å) and angles (°) for [Ru(dmp)₂-(OBIP)](OH)(ClO₄)·CH₃CN **1**

Ru–N(1)	2.110(2)	Ru–N(4)	2.096(2)
Ru–N(2)	2.092(2)	Ru–N(5)	2.073(2)
Ru–N(3)	2.096(2)	Ru–N(6)	2.079(2)
N(1)–Ru–N(2)	79.54(10)	N(5)–Ru–N(6)	78.88(8)
N(1)–Ru–N(3)	178.45(9)	Ru–N(1)–C(1)	130.7(2)
N(1)–Ru–N(4)	101.90(9)	Ru–N(1)–C(12)	109.9(2)
N(1)–Ru–N(5)	98.65(9)	Ru–N(2)–C(10)	130.9(2)
N(1)–Ru–N(6)	82.24(9)	Ru–N(2)–C(11)	111.30(19)
N(2)–Ru–N(3)	100.19(9)	Ru–N(3)–C(15)	132.12(19)
N(2)–Ru–N(4)	94.56(9)	Ru–N(3)–C(26)	110.66(18)
N(2)–Ru–N(5)	173.18(8)	Ru–N(4)–C(24)	130.9(2)
N(2)–Ru–N(6)	94.34(8)	Ru–N(4)–C(25)	111.09(17)
N(3)–Ru–N(4)	79.63(9)	Ru–N(5)–C(38)	128.32(18)
N(3)–Ru–N(5)	81.43(9)	Ru–N(5)–C(39)	114.91(16)
N(3)–Ru–N(6)	96.27(9)	Ru–N(6)–C(29)	128.90(19)
N(4)–Ru–N(5)	92.25(8)	Ru–N(6)–C(40)	113.96(16)
N(4)–Ru–N(6)	170.74(8)		
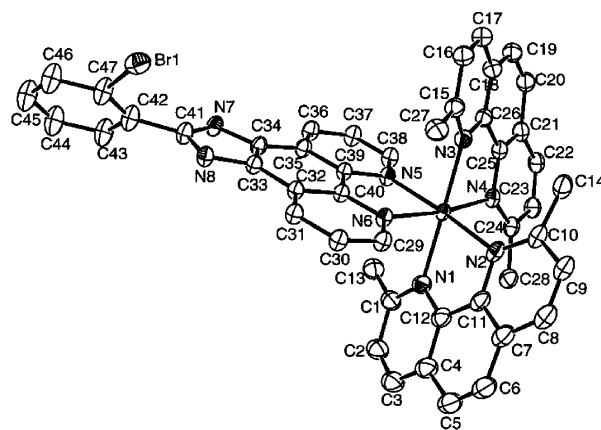
Fig. 1 An ORTEP drawing of [Ru(dmp)₂(OBIP)]²⁺ and the atom numbering.

[Ru(dmp)₂(OBIP)]²⁺ cation, a disordered ClO₄⁻, a OH⁻ and an acetonitrile molecule. The OH⁻ anion forms a hydrogen bond with the imidazole nitrogen (N7). An ORTEP drawing of the cation with atomic numbering scheme is depicted in Fig. 1. Selected bond lengths and angles are summarized in Table 1. The theoretical calculations for these two complexes have also given some structural parameters which are listed in Table 2.

As shown in Fig. 2, the central Ru(II) atom is chelated by two dmp ligands oriented in a *cis* geometry and a OBIP ligand. The average Ru–N bond length (2.091 Å) is comparable with those published for [Ru(phen)₃]²⁺ (2.063 Å),[24] although there are some differences in size and shape among phen, dmp and OBIP. The coordination geometry about the Ru(II) atom is that of a distorted octahedron, with a bite angle of 79.35° averaged over the three bidentate ligands. Of most interest is the configuration of the expected DNA-intercalating ligand OBIP in the complex. We noticed that, to minimize possible steric interaction between the substituent Br group and the imidazole ring, the 2-bromophenyl group is remarkably twisted with respect to the imidazo[4,5-*f*]-1,10-phenanthroline plane forming a dihedral angle of 48.6°. This twisted conformation has also been confirmed by theoretical calculations, in which this dihedral angle is 48.2°.

For complex **2**, since the Br group substitutes at the *para*-position of the phenyl ring in PBIP, it has a negligible steric influence on the coplanarity of the phenyl containing the *para*-Br group and the imidazo[4,5-*f*]-1,10-phenanthroline moiety in PBIP, the expected DNA-intercalating ligand PBIP should be essentially planar. Results from theoretical calculations show that this dihedral angle is 0.4°. By contrast, in the complex [Ru(phen)₂(OBIP)]²⁺, the computed results show that OBIP is planar and thus phen is not an suitable ancillary ligand

	OBIP or PBIP				dmp			
Compound	Ru–N	N–Ru–N	C–C/C–N	C–Br	Ru–N	N–Ru–N	C–C/C–N	$\phi^a/°$
1	2.126	78.5	1.405	1.962	2.155	79.1	1.407	48.1521
2	2.125	78.5	1.405	1.951	2.156	79.0	1.407	0.4008

^{a} ϕ = Dihedral angle between the benzene and imidazole ring of the intercalative ligand.
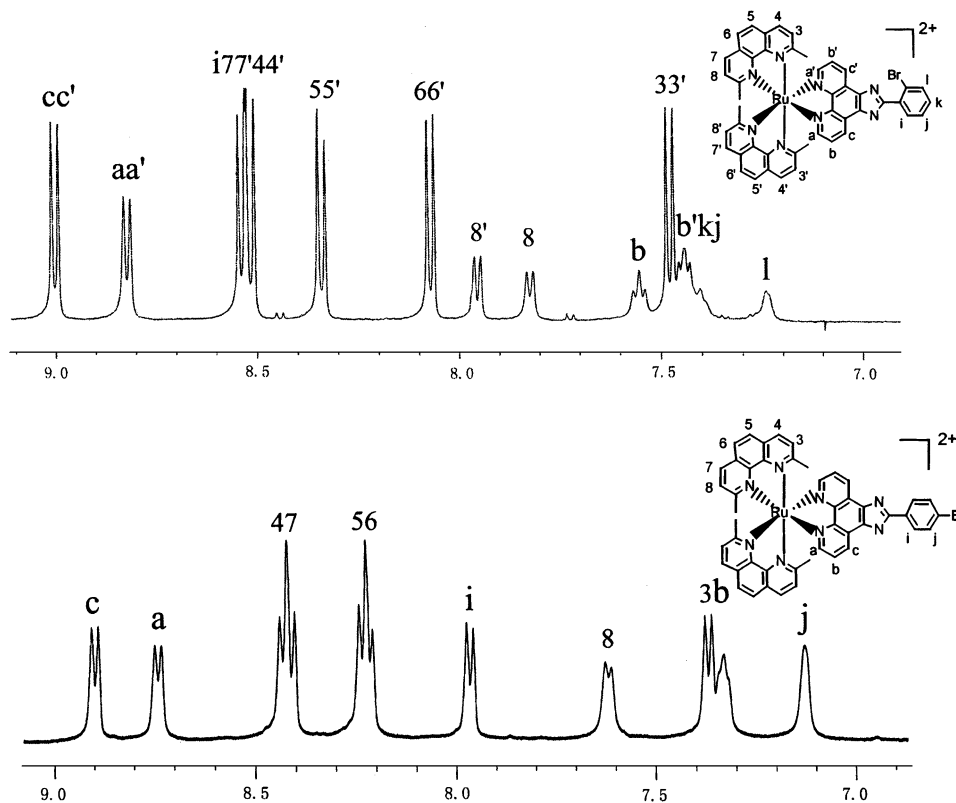
Fig. 2 ^{1}H NMR spectra of the aromatic region of complex **1** (top) and complex **2** (bottom).

to induce non-coplanarity. Our design strategy was thus confirmed by the single crystal X-ray diffraction analysis and theoretical calculations on **1**.

The crystallography as well as DFT calculations of the complexes refer to conditions in the absence of DNA. At the present time, we are not yet able to determine and calculate the structure of a supermolecular system formed from DNA and a complex by crystallography as well as DFT calculations. However, since we have determined and calculated the structures of the complexes in the absence of DNA by reliable methods, it is reasonable to research the trends in DNA-binding of the complexes and analyze the relations between the structures of the free complexes and their DNA-binding properties. Such results should be useful theoretical benchmarks.

^{1}H NMR spectra

The ^{1}H NMR spectra of complexes **1** and **2** are shown in Fig. 2. Considering the influence of steric, inductive and conjugative effects sytematically and comparing them with those of similar compounds,[25] all proton resonance signals of the aromatic region are assigned and given in Fig. 2. For each of the two complexes, two sets of NMR signal were observed. One set corresponds to the dmp ligand, and the other set corresponds to the OBIP or PBIP ligand. Both the two complexes display approximate C_{2v} symmetry in solution, and the two dmp ligands and the two halves of OBIP or PBIP have nearly the same chemical and magnetic environment. On the other hand,
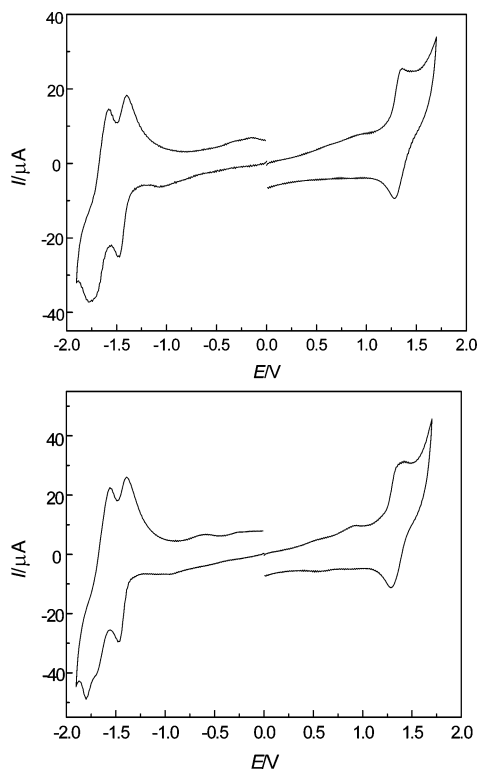
owing to the repulsive interaction between two methyl substituents of each dmp ligand, along with the consideration that the PBIP ligand in complex **2** is more symmetrical than the OBIP ligand in complex **1**, the chemical shifts of the protons located in the phenanthroline ring of dmp are totally split in complex **1** but only partially split in complex **2**. The proton resonance signals of the phenanthroline moiety for the OBIP ligand in complex **1** appear to more downfield in comparison with those of PBIP ligand in complex **2**. This relates to the structure of the ligands. Since the conformation of the OBIP ligand in complex **1** is twisted by 48.6°, the protons located in the phenanthroline moiety of OBIP ligand suffer a stronger π-attraction from N atoms with greater electronegativity, and thus these protons possess more positive charge. As a result they are more downfield shifted.

Electrochemistry

The electrochemical behavior of the two complexes have been studied in acetonitrile. The cyclic voltammetric (CV) behavior of complexes **1** and **2** are shown in Fig. 3. Each complex exhibits well shaped oxidation (one) and reduction (two) waves in the sweep range from −1.9 to +1.7 V, the half-wave potentials $E_{1/2}$, taken as the average of the cathodic peak potential E_{pc} and the anodic peak potential E_{pa}, being −1.671, −1.438 and 1.322 V vs. SCE for [Ru(dmp)$_2$(OBIP)]$^{2+}$ and −1.681, −1.438 and 1.330 V for [Ru(dmp)$_2$(PBIP)]$^{2+}$. A small, poorly shaped reduction wave appears at ca. −1.065 and −1.087 V for [Ru(dmp)$_2$-(OBIP)]$^{2+}$ and [Ru(dmp)$_2$(PBIP)]$^{2+}$, respectively.

Table 3 Some frontier molecular orbital energies (ε_I/atomic unit) of the complexes (1 atomic unit = 27.21 eV)

Compound	Occ	Occ	NHOMO	HOMO	LUMO	Vir	$\Delta\varepsilon_{L-H}$	$\Delta\varepsilon_{L-NH}$
1	−0.3932	−0.3881	−0.3872	−0.3744	−0.2641	−0.2622	0.1103	0.1231
2	−0.3994	−0.3911	−0.3883	−0.3649	−0.2648	−0.2627	0.1001	0.1235

Fig. 3 Cyclic voltammogram of complex **1** (top) and complex **2** (bottom).

Fig. 4 Schematic diagram of energies and related ^{1}MLCT transitions of complexes **1** and **2**.

The electrochemical behavior of Ru(II) polypyridyl complex has been rationalized in terms of a metal-based oxidation and a series of reductions, which are based on the ligands and occur in a stepwise manner for each π* system.[26] As expected, the oxidation potential of [Ru(dmp)$_2$(PBIP)]$^{2+}$ is 8 mV more positive than that of [Ru(dmp)$_2$(OBIP)]$^{2+}$. The phenyl ring containing the *para*-Br group is coplanar with the imidazo-[4,5-*f*]-1,10-phenanthroline moiety in PBIP, which expands the π-delocalization and thus decreases the σ-donor capacity of PBIP, leading to a decrease of the electron density on the Ru ion, and in turn stabilizes the metal d$_\pi$ orbital.[27] As a result, the oxidation potential shifts more positively. The first reduction, which depends on the ligand predominantly populated by the lowest unoccupied molecular orbital (LUMO),[26] is proposed to occur at PBIP or OBIP, and appears irreversible, making a comparison between the two complexes difficult. The latter two successive reductions are characteristic of the two dmp ligands.[26]

The above-mentioned electrochemical trends can be also explained by our theoretical results. Some computed frontier MO energies, schematic diagram of energies, and the related orbital stereographs of the two complexes are given in Table 3, Fig. 4 and Fig. 5, respectively. From Fig. 5, we can see that the MO characterized by metal d-orbitals in the occupied frontier MO is the NHOMO instead of HOMO, so that the oxidation of the central metal should happen on the NHOMO. Since the NHOMO energy of complex **2** is lower than that of complex **1** (see Table 3 and Fig. 4), its oxidation potential is more positive than that of the latter. On the other hand, since the LUMO is playing an electron-accepting role, and the LUMO energy of complex **2** is also lower than that of complex **1**, the reduction potential of the former is more negative than that of the latter.
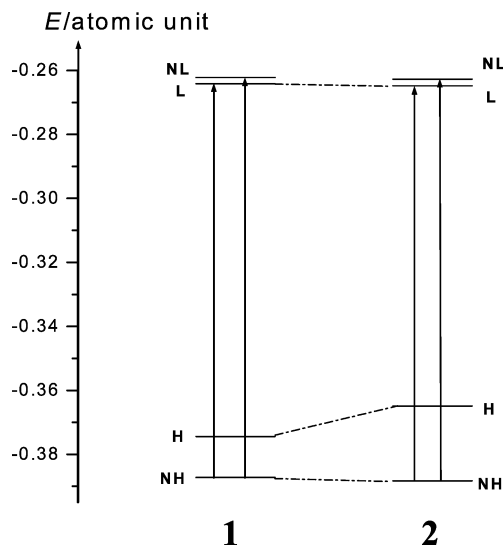
Absorption spectroscopic studies

The electronic absorption spectra of complexes **1** and **2** mainly consist of two resolved bands. The low energy absorption band centered at ~470 nm is assigned to a metal-to-ligand charge transfer (MLCT) transition and the other band centered at ~270 nm is attributed to an intraligand (IL) π–π* transition by comparison with the spectra of other polypyridyl Ru(II) complexes.[21] The electronic spectral traces of the two complexes titrated with DNA are shown in Fig. 6. As the DNA concentration is increased, for complex **1**, the hypochromism in the IL band reaches as high as 15.9% at 269 nm with a red shift of 1 nm at a ratio of [DNA]/[Ru] of 9. The MLCT band at 465 nm shows hypochromism by about 7.7% and a red shift of 2 nm under the same experimental conditions. For complex **2**, upon addition of DNA, the IL band at 271 nm exhibits hypochromism of about 26.0% with a 4 nm red shift at a ratio of [DNA]/[Ru] of 6. Although the MLCT band at 466.0 nm shows no obvious hypochromism, a red shift of 9 nm in the MLCT band is observed under the same experimental conditions. Comparing the hypochromism of the two complexes with that of their parent complex [Ru(phen)$_3$]$^{2+}$ (hypochromism of 12% in the MLCT band at 445 nm and red shift of 2 nm),[28] which interacts with DNA through a semi-intercalation or quasi-intercalation,[3f] and considering that the absorption spectrum of [Ru(bpy)$_3$]$^{2+}$, a typical electrostatic binding complex, was demonstrated to be unchanged upon the addition of the DNA,[5a] these spectral characteristics obviously suggest that the two complexes in our paper interact with DNA most likely through a mode that involves a stacking interaction between the aromatic chomophore and the base pairs of DNA. The spectra also imply that complex **2** binds to DNA more strongly than complex **1**.

To compare quantitatively the affinity of the two complexes towards DNA, the intrinsic binding constants K_b of the two complexes to CT DNA were determined by monitoring the changes of absorbance in the IL band with increasing concentration of DNA. The intrinsic binding constant K_b of complexes **1** and **2** obtained were *ca.* 1.18×10^4 and 3.12×10^4 M^{-1}, respectively, from the decay of the absorbances. Comparing the intrinsic binding constant of the two complexes with those of
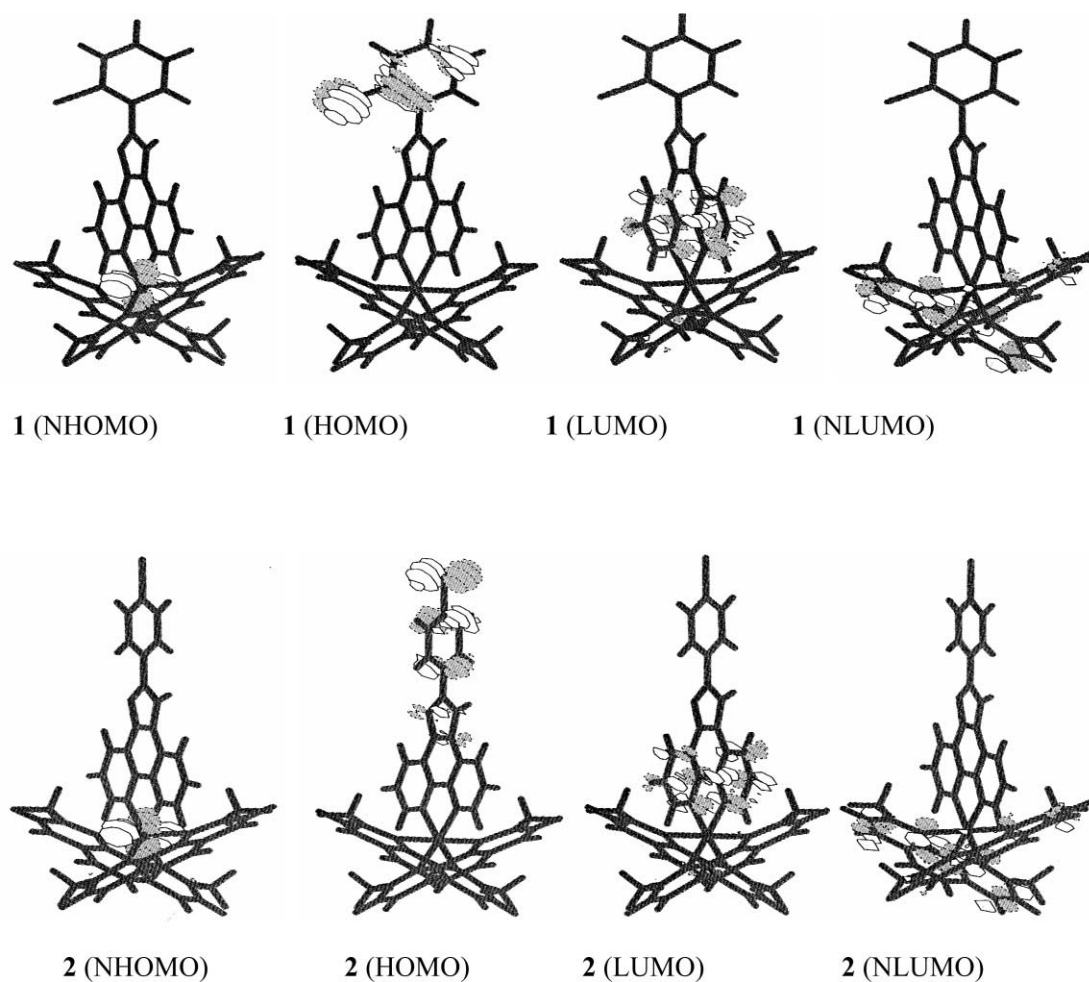
1 (NHOMO)   1 (HOMO)   1 (LUMO)   1 (NLUMO)

2 (NHOMO)   2 (HOMO)   2 (LUMO)   2 (NLUMO)

Fig. 5 Some related frontier molecular orbital stereographs of complexes **1** and **2**.

DNA-intercalative Ru(II) complexes (1.1×10^4–4.8×10^4 M^{-1})[29] and the parent complex [Ru(phen)$_3$]$^{2+}$ (5.5×10^3 M^{-1}),[7b] we can deduce that complex **2** binds strongly to DNA by intercalation and complex **1** is on the border of classical intercalation and near non-classical intercalation to DNA. The better binding of complex **2** to DNA than that of complex **1** can be explained by the the better planarity of the PBIP ligand in complex **2** than that of OBIP ligand in complex **1**. The intrinsic binding constants of both the complexes are smaller than that of [Ru-(dmp)$_2$(HPIP)]$^{2+}$ {HPIP = 2-(2-hydroxyphenyl)imidazo[4,5-*f*]-1,10-phenanthroline} (4.0×10^5 M^{-1}),[30] and much smaller than that of [Ru(dmp)$_2$(dppz)]$^{2+}$ (dppz = dipyridophenazine) (2.3×10^6 M^{-1}).[31] This can also be interpreted by the planarity of the intercalated ligand. For the HPIP ligand, the *ortho* phenolic group of HPIP could be closely coplanar with the imidazole ring due to the formation of an intramolecular hydrogen bond with the nitrogen atom of the imidazole ring.[32] The planar area and the size of the extended π system for the intercalated ligands is in the order of dppz > HPIP > PBIP > OBIP. In general, extension of the intercalative ligand planarity will increase the strength of interaction of the complexes with DNA.[33]

Some trends in electronic absorption spectra can be explained by the theoretical results. From Fig. 5, we have seen that the MO characterized by metal d-orbitals in the occupied frontier MO is NHOMO instead of HOMO, so that the λ_{max} of the ^{1}MLCT spectral band should be assigned to the electron transition from the NHOMO to the LUMO. Such an assignment can be confirmed by the fact that the wavelength corresponding to the theoretical maximum of the ^{1}MLCT spectral band agrees well with the experimental value. According to the approximate correlation of the reverse ratio of the energy difference ($\Delta\varepsilon_{L-NH}$) between the LUMO and the NHOMO to

the experimental wavelength (λ_{max}), using $\Delta\varepsilon_{L-H}$ data of related complexes in Table 3 and selecting the parent complex [Ru(bpy)$_3$]$^{2+}$ as the standard ($\lambda_{max} = 452$, $\Delta\varepsilon_{L-H} = 0.1239$ atomic unit),[34] we can evaluate the wavelengths λ_{max} of the ^{1}MLCT bands of complexes **1** and **2** to be ~455 nm, *cf.* the experimental value of ~465 nm. In addition, the binding constant K_b (**2**) > K_b (**1**) can be also explained by the fact that the LUMO energy (-0.2648 atomic unit) of complex **2** is lower than that (-0.2641 atomic unit) of complex **1**. A lower LUMO energy is advantageous to accept the electrons from base pairs of DNA in intercalative mode according to frontier molecular orbital theory.

Fluorescence spectroscopic studies

For both the complexes, no emission was observed either in Tris buffer or in the presence of CT DNA. This could be caused by vibronic coupling between the methyls of the 2,9-dimethyl-1,10-phenanthroline ligand and solvent, leading to dissipation of energy in a non-radiative process. Similar results have observed for this type of Ru(II) complexes.[30,31]

Steady-state competitive binding experiments using complexes **1** and **2** as quenchers may give further information about the binding of the two complexes to DNA. Ethidium bromide (EB) emits intense fluorescence light in the presence of DNA, due to its strong intercalation between adjacent DNA base pairs. It was previously reported that the enhanced fluorescence can be quenched, at least partially, by the addition of a second molecule.[16,35] The quenching extent of fluorescence of EB bound to DNA is used to determine the extent of binding of the second molecule to DNA. The emission spectra of EB bound to DNA in the absence and the presence of both the complexes are shown in Fig. 7. The addition of complexes **1** and
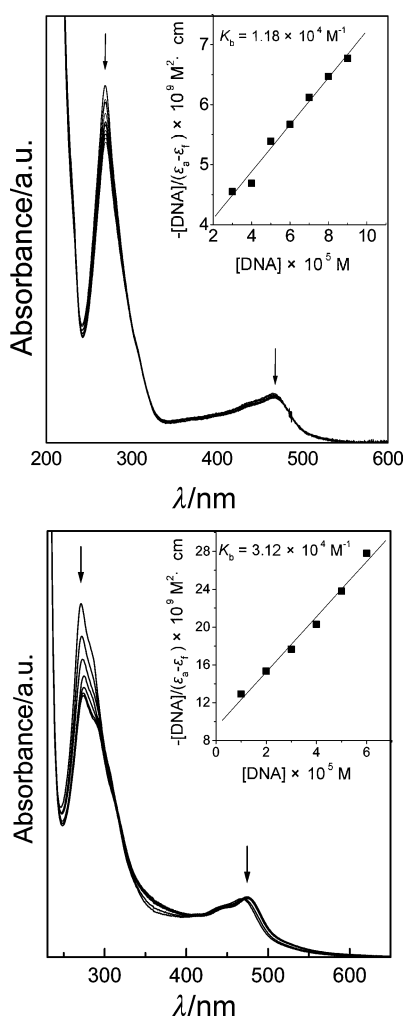
Fig. 6 Absorption spectral of complex **1** (top, [Ru] = 10 μM; [DNA]/[Ru] = 0, 1, 2, 3, 4, 5, 6, 7, 8, 9) and complex **2** (bottom, [Ru] = 10 μM; [DNA]/[Ru] = 0, 1, 2, 3, 3, 5, 6) in Tris-HCl buffer upon addition of CT DNA with subtraction of the DNA absorbance. The arrows show the absorbance changes upon increasing DNA concentrations. Inset: plots of [DNA]/($\varepsilon_a - \varepsilon_f$) *vs.* [DNA] for the titration of DNA with complexes; ■, experimental data points; full line, linear fitting of the data.

2 to DNA, pretreated with EB, causes appreciable reduction in emission intensity of 59.4 and 38.4% relative to that observed in the absence of complexes **1** and **2** at a ratio of [Ru]/[EB] of 1.25. This indicates that the two complexes compete with EB in binding to DNA and that DNA-binding of complex **2** is stronger than that of complex **1**.
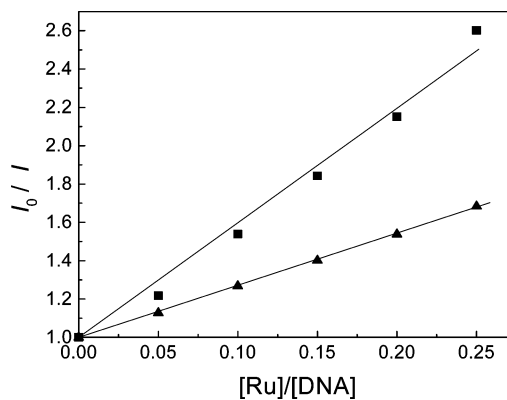
The fluorescence quenching curves of DNA-bound EB by complexes **1** and **2** are shown in Fig. 8. The quenching plots illustrate that the quenching of EB bound to DNA by both complexes are in good agreement with the linear Stern–Volmer equation. This proves that the two complexes can bind to DNA. The Stern–Volmer constant K values for complexes **1** and complex **2** are 2.72 and 5.98, respectively, reflecting the higher quenching efficiency of complex **2** relative to that of complex **1**. This result suggests DNA-binding of complex **2** is stronger than that of complex **1**. Such a trend is consistent with the previous absorption spectral results.

Viscosity studies

Optical photophysical probes generally provide necessary, but not sufficient clues to support a binding model. Hydrodynamic measurements that are sensitive to length change (*i.e.* viscosity and sedimentation) are regarded as the least ambiguous and most critical tests of a binding model in solution in the absence of crystallographic structural data.[36] A classical intercalation model demands that the DNA helix lengthens as base pairs are
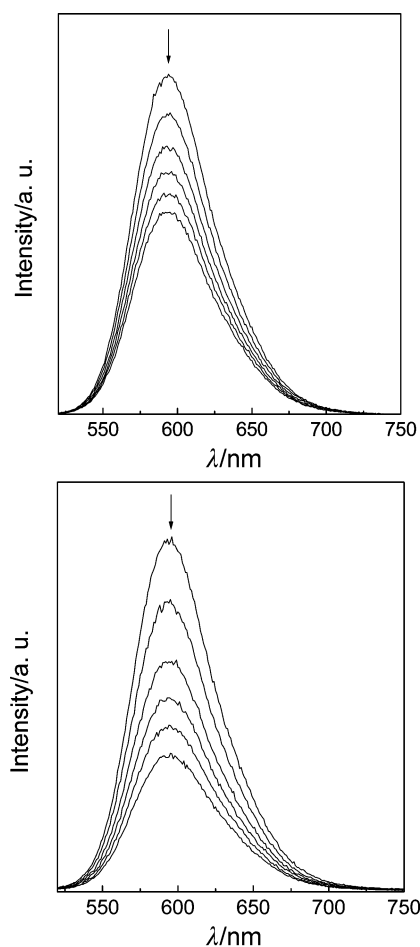

Fig. 7 Emission spectra of EB bound to DNA in presence of complex **1** (top) and complex **2** (bottom). [EB] = 20 μM, [DNA] = 100 μM; [Ru]/[DNA] = 0, 0.05, 0.10, 0.15, 0.20, 0.25. The arrows show the intensity changes upon increasing concentrations of the complexes.

Fig. 8 Fluorescence quenching curve of DNA-bound EB by complex **1** (▲) and complex **2** (■). [EB] = 20 μM, [DNA] = 100 μM; [Ru]/[DNA] = 0, 0.05, 0.10, 0.15, 0.20, 0.25.

separated to accommodate the bound ligand, leading to the increase of DNA viscosity. In contrast, a semi-intercalation of complex such as Δ-[Ru(phen)₃]²⁺ could bend (or kink) the DNA helix, reduce its effective length and, concomitantly, its viscosity.[3f,36] In addition, some complexes such as [Ru(bpy)₃]²⁺, which interacts with DNA by an electrostatic binding mode, have no influence on DNA viscosity.[32]

The effects of complexes **1** and **2** on the viscosity of DNA are shown in Fig. 9. The viscosity of DNA decreases with increasing concentration of complex **1**. In contrast, as the amount of complex **2** is increased, the relative viscosity of DNA increases steadily. The experimental results suggest that complex **1** binds to DNA by the non-classical semi-intercalation model and
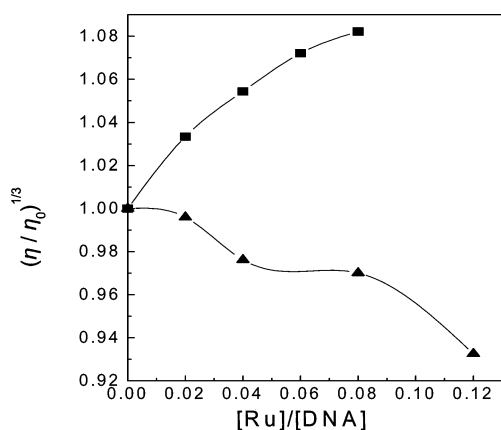
Fig. 9 Effect of increasing amounts of complex **1** (▲) and complex **2** (■) on the relative viscosity of calf thymus DNA at 28.0 ± 0.1 °C. [DNA] = 0.5 mM.

complex **2** binds to DNA through a classical intercalation mode. This difference of DNA-binding mode between complexes **1** and **2** should be caused by the different planarity of the two complexes. For complex **1**, owing the steric constraint of the *ortho*-Br group in the phenyl ring, the imidazo[4,5-*f*]-1,10-phenanthroline moiety is not coplanar with the 2-bromophenyl ring, and the OBIP ligand can not completely intercalate, at most it could penetrate its substituted phenyl moieties into the DNA base pairs, leaving the other part of the ligand in the groove. The semi-intercalation may act as a "wedge" to pry apart one side of a base-pair stack, as observed for Δ-[Ru(phen)$_3$]$^{2+}$,[3f,36] but not fully separate the stack as required by the classical intercalation mode. This would cause a static bend or kink in the helix and decrease the viscosity of DNA. For complex **2**, the intercalated PBIP ligand is essentially planar, and can intercalate deeply and tightly into adjacent DNA base pairs. This would cause an extension in the helix and increase the viscosity of DNA.

Enantioselective binding

According to the proposed binding model,[37] the Δ enantiomer of the complex, a right-handed propeller-like structure, will display a greater affinity than the Λ enantiomer with the right-handed calf thymus DNA helix, due to the appropriate steric matching. The enantiospecific binding of a complex to DNA can be observed clearly from circular dichroism spectra.

The CD spectra in the UV region of the two complexes after their racemic solution have been dialysed against CT DNA are shown in Fig. 10. The presence of CD signals indicates enrichment of the isomer binding less favorably to DNA. The
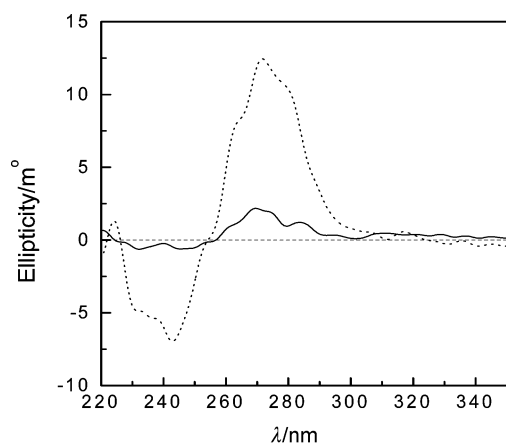
Fig. 10 Circular dichroism spectra of the dialysates of complex **1** (full lines) and complex **2** (dotted lines) after 48 h dialysis against calf thymus DNA ([Ru] = 100 μM, [DNA] = 1.0 mM).

dialysate for complex **1** (full lines) shows two CD signals with a positive peak at 270.6 nm and a negative peak at 246.7 nm, while complex **2** (dotted lines) shows strong CD signals with a positive peak at 271.2 nm and a negative peak at 243.0 nm, respectively. That the CD signals of complex **2** are much stronger than those of complex **1** is explained by the fact that complex **2** binds to DNA more strongly than complex **1**.

Although neither of the two complexes have been resolved into their pure enantiomers, and we can not determine which enantiomer binds to DNA enantioselectively for each of the two complexes, it is certain that both the two complexes interact with CT DNA enantioselectivly, and that complex **2** is a much better candidate for an enantioselective binder to CT DNA than complex **1**.

Conclusions

The structure of complex **1** has been determined by single-crystal X-ray diffraction techniques. The imidazo[4,5-*f*]-1,10-phenanthroline moiety is not coplanar with the 2-bromophenyl ring, having a dihedral angle of 48.6° in OBIP. The twisted conformation has been further confirmed by theoretical calculations applying the density functional theory (DFT) method, in which this dihedral angle is 48.2°. The theoretical calculations also show that the PBIP ligand in complex **2** is essentially planar (the dihedral angle is 0.4°). The experimental results show that while complex **1** binds to CT DNA *via* a semi-intercalative mode, complex **2** can strongly bind to CT DNA through intercalation, and thus complex **2** is a much better candidate as an enantioselective binder to CT DNA than complex **1**. Some experimental regularities or trends can also be explained reasonably by the theoretical calculations. All of these further suggest that the planarity of the intercalated ligand has a significant effects on the spectral properties, the DNA-binding behavior and other properties of the complexes, and that the density functional theory (DFT) method can be used to explain and predict some regularities or trends in the interaction of the polypyridyl Ru(II) complexes with DNA.

Acknowledgements

References

1 L.-N. Ji, X.-H. Zou and J.-G. Liu, *Coord. Chem. Rev.*, 2001, **216–217**, 513.

2 S. O. Kelle, G. Orellana and J. K. Barton, *J. Photochem. Photobiol. B*, 2000, **58**, 72; E. D. Stemp and J. K. Barton, *Inorg. Chem.*, 2000, **39**, 3868.

3 (*a*) J. Olofsson, B. Onfelt, P. Lincoln, B. Norden, P. Matousek, A. W. Parker and E. Tuite, *J. Inorg. Biochem.*, 2002, **91**, 286; (*b*) C. G. Coates, J. Olofsson, M. Coletti, J. J. McGarvey, B. Onfelt, P. Lincoln, B. Norden, E. Tuite, P. Matousek and A. W. Parker, *J. Phys. Chem. B*, 2001, **105**, 12653; (*c*) B. Onfelt, P. Lincoln, B. Norden, J. S. Baskin and A. H. Zewail, *Proc. Natl. Acad. Sci. USA*, 2000, **97**, 5708; (*d*) K. Gisselfalt, P. Lincoln, B. Norden and M. Jonsson, *J. Phys. Chem. B*, 2000, **104**, 3651; (*e*) K. Vickery, R. Vagg, P. Lincoln, B. Norden and M. Eriksson, *J. Biomol. Struct. Dyn.*, 1999, **17**, 519; (*f*) P. Lincoln and B. Norden, *J. Phys. Chem. B*, 1998, **102**, 9583.

4 B. Onfelt, L. Gostring, P. Lincoln, B. Norden and A. Onfelt, *Mutagenesis*, 2002, **17**, 317; C. M. Dupureur and J. K. Barton, *Inorg. Chem.*, 1997, **36**, 33; I. Greguric, J. R. Aldrich-Wright and J. G. Collins, *J. Am. Chem. Soc.*, 1997, **119**, 3621; R. B. Nair, E. S. Teng, S. L. Kirkland and C. J. Murphy, *Inorg. Chem.*, 1998, **37**, 139; J.-G. Liu, B.-H. Ye, H. Li, L.-N. Ji, R.-H. Li and J.-Y. Zhou, *J. Inorg. Biochem.*, 1999, **73**, 117.

5 (*a*) G. Yang, J.-Z. Wu, L. Wang, L.-N. Ji and X. Tian, *J. Inorg. Biochem.*, 1997, **66**, 141; (*b*) G. Yang, L. Wang and L.-N. Ji, *J. Inorg. Biochem.*, 1997, **67**, 289.

6 J.-Z. Wu, L. Li, T.-X. Zeng, L.-N. Ji, J.-Y. Zhou and R.-H. Li, *Polyhedron*, 1997, **16**, 103; J.-Z. Wu, B.-H. Ye, L. Wang, L.-N. Ji, J.-Y. Zhou, R.-H. Li and Z.-Y. Zhou, *J. Chem. Soc., Dalton Trans.*, 1997, **21**, 1395.

7 (*a*) B. M. Goldstein, J. K. Barton and H. M. Berman, *Inorg. Chem.*, 1986, **25**, 842; (*b*) A. M. Pyle, J. P. Rehmann, R. Meshoyrer, C. V. Kumar, N. J. Turro and J. K. Barton, *J. Am. Chem. Soc.*, 1989, **111**, 3051; (*c*) Y. Xiong, X.-F. He, X.-H. Zou, J.-Z. Wu, X.-M. Chen, L.-N. Ji, R.-H. Li, J.-Y. Zhou and K.-B. Yu, *J. Chem. Soc., Dalton Trans.*, 1999, **23**, 19; (*d*) R. J. Morgan, S. Chatterjee, A. D. Baker and T. C. Strekas, *Inorg. Chem.*, 1991, **30**, 2687.

8 F. Liu, K. A. Meadows and D. R. McMillin, *J. Am. Chem. Soc.*, 1993, **115**, 6699; G. Yang, J.-Z. Wu, L. Wang, T.-X. Zeng, L.-N. Ji and X. Tian, *Chin. Chem. Lett.*, 1996, **7**, 1127; Q.-X. Zhen, Q.-L. Zhang, J.-G. Liu, B.-H. Ye, L.-N. Ji and L. Wang, *J. Inorg. Biochem.*, 2000, **78**, 293.

9 P. Hohenberg and W. Kohn, *Phys. Rev. B*, 1964, **136**, 864; A. D. Becke, *J. Chem. Phys.*, 1993, **98**, 1372; A. Gorling, *Phys. Rev. A*, 1996, **54**, 3912; J. B. Foresman and Æ. Frisch, *Exploring Chemistry with Electronic Structure Methods*, Gaussian Inc., Pittsburgh PA, 2nd edn., 1996.

10 J. P. Collin and J. P. Sauvage, *Inorg. Chem.*, 1986, **25**, 135; W. Paq and R. Eisenberg, *Inorg. Chem.*, 1997, **36**, 2287.

11 Y. Xiong, X.-H. Zou, J.-Z. Wu, L.-N. Ji, R.-H. Li, J.-Y. Zhou and K.-B. Yu, *Transition Met. Chem.*, 1999, **24**, 263.

12 G. M. Sheldrick, SHELXTL 97, Program for X-Ray Crystal Structure Refinement, Göttingen University, 1997.

13 J. Marmur, *J. Mol. Biol.*, 1961, **3**, 208.

14 M. E. Reichmann, S. A. Rice, C. A. Thomas and P. Doty, *J. Am. Chem. Soc.*, 1954, **76**, 3047.

15 A. Wolfe, G. H. Shimer and T. Meehan, *Biochemistry*, 1987, **26**, 6392.

16 J. R. Lakowicz and G. Webber, *Biochemistry*, 1973, **12**, 4161.

17 J. B. Chaires, N. Dattagupta and D. M. Crothers, *Biochemistry*, 1982, **21**, 3933.

18 G. Cohen and H. Eisenberg, *Biopolymers*, 1969, **8**, 45.

19 C. V. Kumar, J. K. Barton and N. J. Turro, *J. Am. Chem. Soc.*, 1985, **107**, 5518.

20 P. J. Hay and W. R. Wadt, *J. Chem. Phys.*, 1985, **82**, 270; P. J. Hay and W. R. Wadt, *J. Chem. Phys.*, 1985, **82**, 299.

21 A. Juris, V. Balzani, F. Barigelletti, Campagna, S. Campagna, P. Belser and A. V. Zelewsky, *Coord. Chem. Rev.*, 1988, **84**, 85.

22 M. J. Frisch, G. W. Trucks, H. B. Schlegel, G. E. Scuseria, M. A. Robb, J. R. Cheeseman, V. G. Zakrzewski, J. A. Montgomery, Jr. R. E. Stratmann, J. C. Burant, S. Dapprich, J. M. Millam, A. D. Daniels, K. N. Kudin, M. C. Strain, O. Farkas, J. Tomasi, V. Barone, M. Cossi, R. Cammi, B. Mennucci, C. Pomelli, C. Adamo, S. Clifford, J. Ochterski, G. A. Petersson, P. Y. Ayala, Q. Cui, K. Morokuma, N. Rega, P. Salvador, J. J. Dannenberg, D. K. Malick, A. D. Rabuck, K. Raghavachari, J. B. Foresman, J. Cioslowski, J. V. Ortiz, A. G. Baboul, B. B. Stefanov, G. Liu, A. Liashenko, P. Piskorz, I. Komaromi, R. Gomperts, R. L. Martin, D. J. Fox, T. Keith, M. A. Al-Laham, C. Y. Peng, A. Nanayakkara, M. Challacombe, P. M. W. Gill, B. Johnson, W. Chen, M. W. Wong, J. L. Andres, C. Gonzalez, M. Head-Gordon, E. S. Replogle and J. A. Pople, *Gaussian 98*, Revision A.11.4, Gaussian, Inc., Pittsburgh PA, 2002.

23 G. Schaftenaar, Molden v3.6 program, CMBI, Faculty of Science, University of Nijmegen, 1999.

24 J. Bueu and A. J. Stoll, *Acta Crystallogr., Sect. C*, 1996, **52**, 1174.

25 Q.-X. Zhen, B.-H. Ye, J.-G. Liu, Q.-L. Zhang, L.-N. Ji and L. Wang, *Inorg. Chim. Acta*, 2000, **303**, 141; X.-H. Zou, B.-H. Ye, H. Li, J.-G. Liu, Y. Xiong and L.-N. Ji, *J. Chem. Soc., Dalton Trans.*, 1999, **23**, 1423.

26 B. K. Ghosh and A. Chakra-Vorty, *Coord. Chem. Rev.*, 1989, **95**, 239.

27 D. P. Rillema, G. Allen, T. J. Meyer and D. C. Conrad, *Inorg. Chem.*, 1983, **22**, 1617.

28 Y. Xiong and L.-N. Ji, *Coord. Chem. Rev.*, 1999, **185–186**, 711.

29 X.-H. Zou, B.-H. Ye, H. Li, Q.-L. Zhang, H. Chao, J.-G. Liu, L.-N. Ji and X.-Y. Li, *J. Biol. Inorg. Chem.*, 2001, **6**, 143.

30 J.-G. Liu, Q.-L. Zhang, L.-N. Ji, Y.-Y. Cao and X.-F. Shi, *Transition Met. Chem.*, 2001, **26**, 733.

31 J.-G. Liu, Q.-L. Zhang, X.-F. Shi and L.-N. Ji, *Inorg. Chem.*, 2001, **40**, 5045.

32 J.-G. Liu, B.-H. Ye, H. Li, Q.-X. Zhen, L.-N. Ji and Y.-H. Fu, *J. Inorg. Biochem.*, 1999, **76**, 265.

33 Y. Xiong and L.-N. Ji, *Coord. Chem. Rev.*, 1999, **189**, 1–23.

34 K.-C. Zheng, J.-P. Wang, W.-L. Peng, X.-W. Liu and F.-C. Yun, *J. Phys. Chem. A*, 2001, **105**, 10899.

35 B. C. Baguley and M. Lebret, *Biochemistry*, 1984, **23**, 937.

36 S. Satyanarayana, J. C. Dabrowiak and J. B. Chaires, *Biochemistry*, 1992, **31**, 9319; S. Satyanarayana, J. C. Dabrowiak and J. B. Chaires, *Biochemistry*, 1993, **32**, 2573.

37 J. K. Barton and A. L. Raphael, *J. Am. Chem. Soc.*, 1984, **106**, 2172; J. K. Barton, *Science*, 1986, **233**, 727; A. M. Pyle and J. K. Barton, *Prog. Inorg. Chem.*, 1990, **38**, 413.